5-2023

Neuronal or Intestinal Knockdown of C. elegans nadk-1 Decreases Oxygen Consumption and Reactive Oxygen Species

Jake Regan
East Tennessee State University

Neuronal or Intestinal Knockdown of *C. elegans nadk-1* Decreases Oxygen Consumption and Reactive Oxygen Species

---

A thesis

presented to

The faculty of the Department of Biology

East Tennessee State University

In partial fulfillment

of the requirements for the degree

Master of Science in Biology

---

by

Jake A. Regan

May 2023

Dr. Patrick Bradshaw

Dr. Tyrone Genade

Dr. Chad Frasier

Keywords: NAD kinase, NADPH, *Caenorhabditis elegans*, peroxide, thioredoxin reductase

ABSTRACT

Neuronal or Intestinal Knockdown of *C. elegans nadk-1* Decreases Oxygen Consumption and Reactive Oxygen Species

by

Jake A. Regan

Reactive oxygen species (ROS) such as H_2O_2 can damage cellular components and are formed as a byproduct of mitochondrial oxidative metabolism. Studies using the nematode *C. elegans* have found that increasing ROS during development or early adulthood can extend lifespan, while increasing ROS during later adulthood normally decreases lifespan. NADPH provides the reducing power for several cellular antioxidants and is synthesized in a two-step reaction from NAD^+ with the first step being catalyzed by NAD kinase (NADK). In this study, the effects of knocking down *C. elegans* cytoplasmic NADK, *nadk-1* globally or in a neuron or intestine-specific manner starting from early development on oxygen consumption and ROS levels were determined. Surprisingly, whole body knockdown of *nadk-1* to decrease cytoplasmic NADPH levels decreased oxygen consumption and tert-butyl hydroperoxide-stimulated ROS levels, which was phenocopied by intestine-specific or neuron-specific knockdown. Thioredoxin reductase measurements following *nadk-1* knockdown showed a trend toward increased activity.

DEDICATION

To my family, who taught me to never give up.

AKNOWLEDGEMENTS

I'd like to express my thanks to my advisor and committee chair member, Dr. Patrick Bradshaw, Assistant Professor, Biomedical Sciences Department, East Tennessee State University, for all his help and guidance during my time here.

I would like to thank my committee members Dr. Tyrone Genade and Dr. Chad Frasier for their help and advice.

I would like to thank the ETSU Department of Biology for granting me a GA position while I performed my studies.

I would also like to thank my lab members Leah Jamerson and Mckenzie Peters for their unwavering support and input throughout the course of my research.

TABLE OF CONTENTS

LIST OF FIGURES

CHAPTER 1. INTRODUCTION

Reactive oxygen species (ROS) are a byproduct of aerobic metabolism that can damage cellular components, which is the basis of the long-standing mitochondrial free radical theory of aging (MFRTA) (Bayr 2005). Although primarily produced by the mitochondrial electron transport chain, ROS is also a product of other enzymes such as NADPH oxidases (Nox), mostly present in phagocytes, which produce this ROS as a defense mechanism against pathogenic microorganisms (Babior 2004). Due to its origins in mitochondrial metabolism or immune cells, increased ROS are associated with a number of metabolic disorders including obesity, chronic inflammation, oxidative stress, as well as cancer and cardiovascular disorders (Alfadda and Sallam 2012). The effects of ROS and the resulting oxidative damage on aging and lifespan are of a particular interest. Over the past 15 years some data has been generated that appears to refute the MFRTA such as data showing that increased ROS during development or early adulthood increases lifespan by activating stress response pathways (Liochev 2013).

Cellular Functions of NADPH

Since cells produce ROS as a byproduct of normal metabolism, mechanisms evolved to reduce the ROS production and quench the ROS produced to decrease oxidative damage. The mitochondrial electron transport chain is the major producer of cellular ROS in the form of superoxide (Figure 1). Cytoplasmic and mitochondrial superoxide dismutase enzymes detoxify superoxide into hydrogen peroxide (H_2O_2). The cell has at least three mechanisms to detoxify H_2O_2. Nicotine Adenine Dinucleotide Phosphate (NADP(H)) in the reduced NADPH form functions as a cofactor in two parallel pathways that reduce H_2O_2 into water and molecular oxygen (O_2) (Fernandez-Marcos and Nóbrega-Pereira 2016). Another method to detoxify H_2O_2

is through the use of reduced glutathione (GSH) and the enzyme glutathione peroxidase where the products are H_2O and oxidized glutathione disulfide (GSSG). To reduce GSSG back into two GSH NADPH is oxidized to $NADP^+$ by the enzyme glutathione reductase (Salisbury and Bronas 2015). Peroxiredoxin, thioredoxin, and thioredoxin reductase, the latter which oxidizes NADPH to $NADP^+$ to reduce thioredoxin, constitutes a parallel pathway for the detoxification of H_2O_2. In this pathway peroxiredoxin is first oxidized by H_2O_2, with thioredoxin becoming oxidized when reducing the oxidized peroxiredoxin. The third pathway to detoxify H_2O_2 is through the dismutation of 2 H_2O_2 into $2H_2O + O_2$ by peroxisomal catalase independent of NADPH.

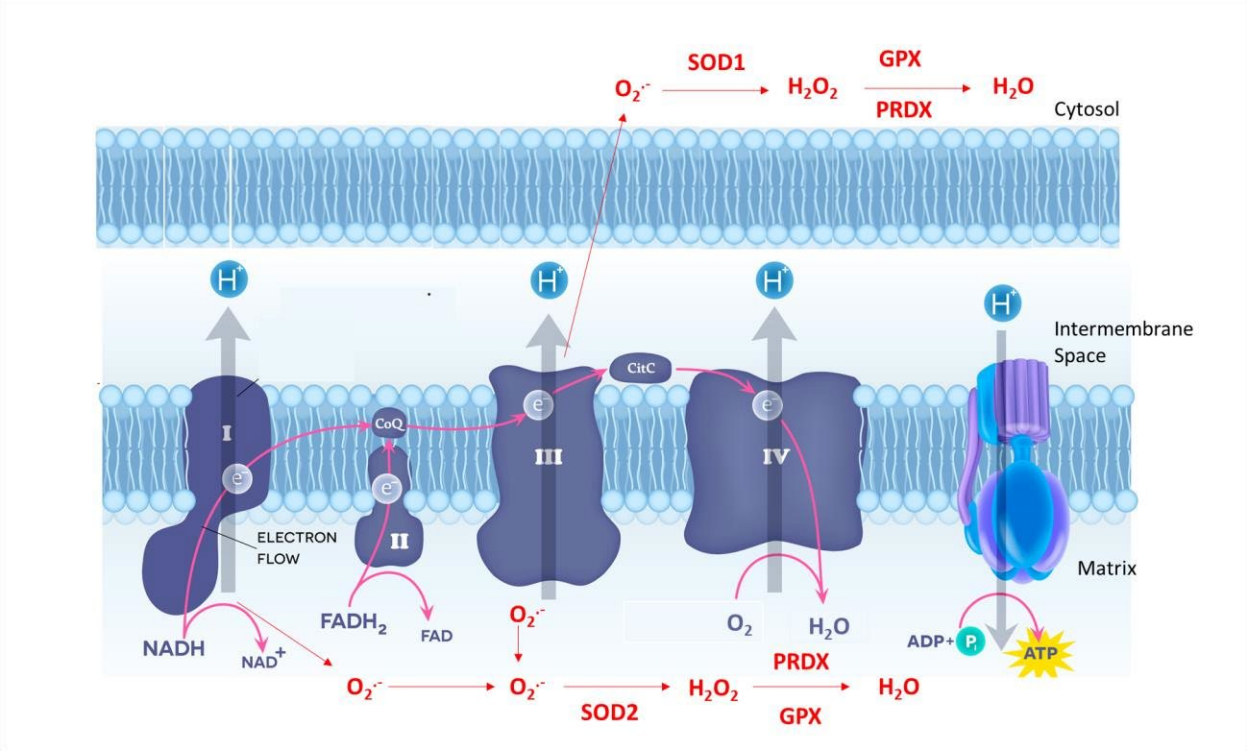

Figure 1. Mitochondrial Electron Transport Chain. The mitochondrial electron transport chain produces ROS in the form of superoxide that is detoxified to H_2O_2 by superoxide dismutase (SOD) and further detoxified to H_2O by glutathione peroxidase (GPX) or peroxiredoxin (PRDX).

NADP(H) has been estimated to be used as a cofactor in roughly 100 human cellular reactions as 426 genes were identified to contain one or more NAD(P) binding sites (Goodman et al. 2018). NADPH is found in nearly all cellular compartments including the cytoplasm, mitochondria, ER, peroxisomes, lysosomes, and the nucleus (Bradshaw 2019). To synthesize $NADP^+$, NAD^+ must be phosphorylated by the enzyme NAD kinase. In mammalian species, there are two genes encoding enzymes with NADK activity, with the first called NADK being localized to the cytoplasm and the second called NADK2 being localized to the mitochondrial matrix. Oddly, the *C. elegans* genome lacks a homolog of NADK and contains two homologous genes to NADK2 called NADK-1 and NADK-2, for the cytoplasmic and mitochondrial localized proteins, respectively (Vickman and Erives 2019; Gong 2021).

In order to maintain the cytoplasmic and mitochondrial ratio of [NADPH]/[[$NADP^+$] close to 100, multiple enzymes are used to convert the majority of cellular $NADP^+$ into NADPH. There are roughly eleven major enzymes that perform this conversion with these enzymes being localized to either the cytoplasm or the mitochondria (Figure 2). The mitochondrial enzymes include isocitrate dehydrogenase 2 (IDH2), malic enzyme 3 (ME3), nicotinamide nucleotide transhydrogenase (NNT), glutamate dehydrogenase (GDH), and ALDH1L2, while the cytoplasmic enzymes are glucose-6-phosphate dehydrogenase (G6PD), 6-phosphogluconate dehydrogenase (6PGD), IDH1, ME1, methylene tetrahydrofolate dehydrogenase 1 (MTHFD1), and ALDH1L1 (Bradshaw 2019). IDH2 is an enzyme of the citric acid cycle that generates NADPH through the reversible oxidative decarboxylation of isocitrate into α-ketoglutarate (Ciccarese and Ciminale 2017). ME1 and ME3 catalyze the oxidative decarboxylation of malate to pyruvate (Ju et al. 2020). NNT uses the mitochondrial proton gradient to reduce $NADP^+$ while oxidizing NADH (Ronchi et al. 2016). Glutamate dehydrogenase is a mitochondrial

enzyme that deaminates glutamate to α-ketoglutarate while reducing $NAD(P)^+$ to NAD(P)H (Z. Xu et al. 2006).

In the liver where pentose phosphate pathway activity (PPP) is extremely low, MTHFD1 and ALDH1L1 synthesize over half of the cytoplasmic NADPH as part of serine catabolism. When formate is not needed to maintain folate cycle flux ALDH1L1 or ALDH1L2 converts 10-formyltetrahydrofolate and $NADP^+$ to CO_2, NADPH, and tetrahydrofolate instead to maintain cellular reducing power (Ju et al., 2020). Both G6PD and 6PGD are enzymes of the oxidative phase of the PPP used for synthesizing ribose for nucleotide metabolism (Patra & Hay, 2014).

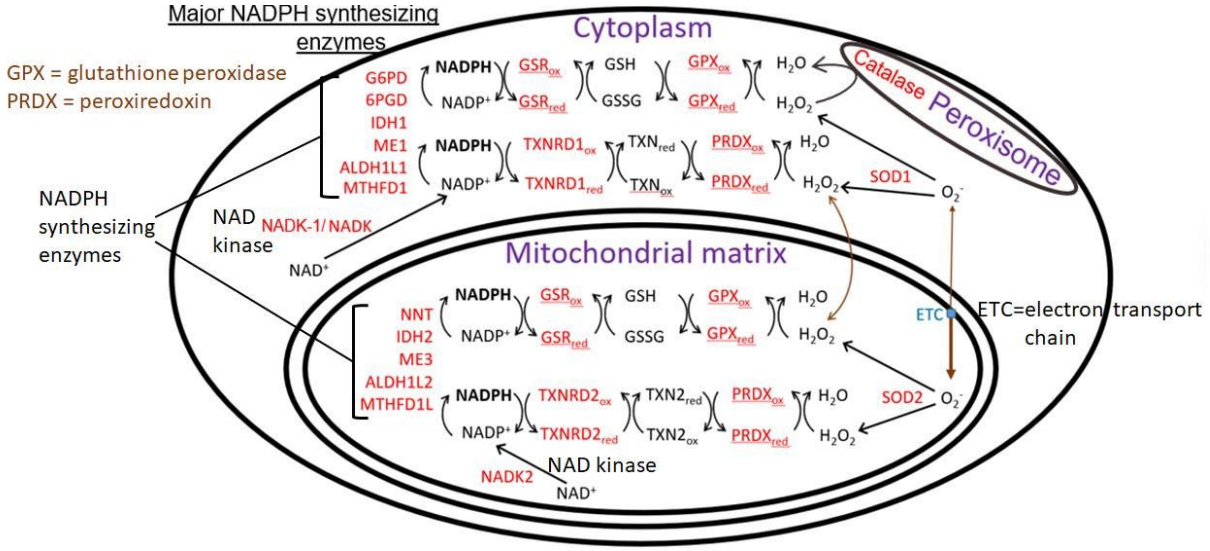

Figure 2. H_2O_2 detoxification pathways. Cytoplasmic and mitochondrial detoxification of H_2O_2 through glutathione peroxidase (GPX), peroxiredoxin (PRDX), and NADPH.

In the mitochondrial matrix, NADPH is oxidized by multiple enzymes such as glutathione reductase and thioredoxin reductase as described above (Fernandez-Marcos ans Nóbrega-Pereira 2016), DECR1, which removes unsaturated fatty acid double bonds so that the fatty acid can be further oxidized by beta-oxidation also oxidizes NADPH (Miinalainen et al.

2009). The bifunctional enzyme AASS (aminoadipate-semialdehyde synthase) catalyzes the first two steps of lysine catabolism, with the second reaction oxidizing NADPH to reduce saccharopine to AAS (aminoadipate-semialdehyde). The enzyme P5CS/ALDH18A1 oxidizes NADPH for the mitochondrial synthesis of proline from glutamate (Zhu et al. 2021) (Nassar et al. 2020) Lastly, the MECR enzyme oxidizes NADPH for mitochondrial fatty acid synthesis, which is required for lipoic acid synthesis and electron transport chain complex stability (Tanvir Rahman et al. 2023). Therefore, human mutation of NADK2 is characterized by accumulation of lysine catabolites, C10:2-carnitine (from defective unsaturated fatty acid beta-oxidation), and lactate (from dysfunctional electron transport chain function that increases mitochondrial NADH and redirects pyruvate to lactate instead of acetyl-CoA) (Zhang and Zhang 2023).

In the cytoplasm NADPH is oxidized by glutathione reductase and thioredoxin reductase in a parallel pathway from that present in the mitochondrial matrix. Cytoplasmic NADPH blocks ferroptosis, a type of necrotic cell death (Ding et al. 2020; Nguyen et al. 2022). Cytoplasmic NADPH is also oxidized for fatty acid and cholesterol synthesis (Foster 2012). Due to the essential role of NADPH in lipid synthesis, knockdown of NADK in *Drosophila* has been shown to lead to an accumulation of the precursors for fatty acid and cholesterol synthesis including acetyl-CoA and citrate (M. Xu et al. 2021). The accumulation of acetyl-CoA led to increased acetylation and inhibition of the PGC-1α homolog *spargel* to decrease mitochondrial biogenesis and O_2 consumption. The decreased fatty acid synthesis also led to decreased levels of cardiolipin required for electron transport chain function (M. Xu et al. 2021). It is also possible that increased citrate could inhibit glycolytic flux, as citrate is known to inhibit phosphofructokinase, the third enzyme of glycolysis, which may lead to decreased pyruvate synthesis and its oxidation by mitochondria contributing to the deficits in mitochondrial

respiration (Chesney 2006). NADPH also plays a role in deoxynucleotide synthesis under normal conditions in dividing cells, as ribonucleotide reductase that converts NMPs to dNMPS oxidizes thioredoxin. As mentioned above thioredoxin can rely on NADPH for reduction to its active form. However, thioredoxin can also be reduced by GSH (Chatterji et al. 2022). Mice with complete hepatic loss of both cytoplasmic glutathione reductase and cytoplasmic thioredoxin reductase were viable due to the increased de novo synthesis of GSH and secretion of GSSG into the extracellular space to maintain the GSH/GSSG ratio (C. G. Miller et al. 2018) So, there appears to be a path for deoxynucleotide and GSH synthesis without oxidizing NADPH, at least in liver. This likely explains the viability of *C. elegans nadk-1* mutants, while mutants of GSH synthesis are nonviable. Alternatively, a splice variant of mitochondrial NADK2 (NADK-2, isoform b) could be targeted to the cytoplasm and maintain the viability of *nadk-1* mutants. In *Drosophila* and higher eukaryotes cytoplasmic NADK knockout is lethal (M. Xu et al. 2021).

With its role in mitochondrial metabolism and ROS detoxification, NADPH is just as important, yet highly understudied when compared to the antioxidant enzymes and metabolites such as vitamin C and vitamin E that use its reducing power to maintain function. Therefore, for my research, I studied the effects of knockdown of *nadk-1*, the *C. elegans* cytoplasmic NADK, on ROS levels. Other rationale for the choice of this project was that knockdown of the PPP enzyme *tald*-1 during larval development increased ROS levels to signal for increased lifespan (Bennett et al. 2017). But a former member of my laboratory found that knockdown of *nadk-1* starting during larval development did not extend lifespan, even though cytoplasmic NADPH levels are likely depleted by either *tald-1* or *nadk-1* knockdown. As ROS during development is known to stimulate pro-longevity stress response pathways, I hypothesized that in contrast to

tald-1 knockdown, *nadk-1* knockdown would not increase ROS levels and this difference is responsible for the normal lifespan following *nadk-1* knockdown.

Mitochondrial Theory of Aging

One of the long-standing theories of aging, the mitochondrial free radical theory of aging (MFRTA), now over 50 years old (Harman 1972), posits that organisms age due to oxidative damage accumulation over time brought on by mitochondrial ROS generation (Chandrasekaran et al. 2017). Cells in young organisms balance ROS production and ROS scavenging to increase the chance of reproduction. In aged organisms, the expression of genes used in antioxidant pathways and other types of cellular repair are downregulated and mitochondrial ROS production is increased, leading to increased ROS and cellular damage, and perhaps leading to aging and aging-related disorders (Braeckman et al. 2002).

Mitohormesis is a process in which exposure to low levels of stress activates a response that leads to increased stress resistance and sometimes increased lifespan. In the case of *C. elegans*, stressors such as heat, starvation, and ROS can induce mitohormesis (Cypser and Johnson, 2002; Bennett et al. 2017). One such way this hormetic response induces lifespan extension is through the activation of the longevity-promoting transcription factor DAF-16, homologous to the four human FOXO genes (Cabreiro et al. 2011). Thus, a nonlethal induction of ROS could lead to an extension of lifespan due to mitohormesis activating lifespan extending transcription factors. Transcription factors such as HLH-30/TFEB and SKN1/Nrf2 have also been shown to be activated by mitohormesis, as they are activated by stresses such as starvation or ROS (Bennett et al. 2017).

Over the last two decades the MFRTA has been rigorously tested leading to some data that refutes its general applicability. For example, some studies using *C. elegans* do not support the MFRTA. The MFRTA predicts that overexpression of superoxide dismutase (SOD), an antioxidant that converts superoxide to H_2O_2, as a first step to combat ROS production, would extend lifespan by decreasing ROS levels. Although SOD (either cytoplasmic *sod-1* or mitochondrial *sod-2*) overexpression did lead to increased longevity (Gladyshev 2014), this was not due to decreased ROS, but due to activation of the longevity-promoting transcription factor DAF-16/FOXO (Cabreiro et al. 2011; Radak et al. 2013). Other studies have shown that knockout of certain antioxidant genes did yield increased ROS, but did not decrease *C. elegans* lifespan (Speakman and Selman, 2011). Likewise, a previous study from my lab showed that knocking down *C. elegans* NADKs (*nadk-1* or *nadk-2*) to decrease NADPH, which is used to reduce many cellular antioxidants, decreased ROS, but did not decrease lifespan as predicted by the MFRTA (Gong 2022). With the accumulating evidence of longevity-promoting effects of ROS during development and early adulthood, newer aging theories have modified the MFRTA to limit its applicability to times of mid-adulthood and beyond.

Redox Systems

As described above, NADPH functioning as a reducing agent has been shown to be a key component of the thiol (GSH and thioredoxin) redox system. This redox system acts as a defense against ROS and consists of proteins such as glutathione peroxidase, glutaredoxin, thioredoxin, peroxiredoxin, and GSH to catalyze the reduction of H_2O_2 into water (Ferguson and Bridge 2019).

GSH, considered to be the primary antioxidant in the thiol system due to its much higher cellular concentration than other thiols, is synthesized by a two-step process. First, the enzyme

glutamate-cystine ligase (GCL) covalently links glutamate and cysteine using a unique nonpeptide bond. The dipeptide is then covalently linked to glycine by the enzyme glutathione synthase to form GSH (Morris et al. 2014). GSH can then be oxidized to GSSG by glutathione peroxidase (GPX) to reduce H_2O_2 to water (Aquilano et al. 2014). In *C. elegans*, the ortholog of the mammalian catalytic subunit of GCL, GCLC, is *gcs-1*, a gene that is induced by the transcriptional regulator SKN-1 (Nrf2 in humans). During oxidative stress, SKN-1 translocates to the nucleus, which upregulates the expression of *gcs-1*. When *gcs-1* expression is upregulated, GSH levels increase to counteract the increased levels of ROS (Oliveira et al. 2009). In cases where *gcs-1* had been knocked down starting from the first day of adulthood, it was surprisingly found that there was increased lifespan and increased resistance to paraquat-induced toxicity (Urban et al. 2017; Ferguson and Bridge, 2019). The reason for the unexpected result was likely a compensatory increase in the expression of the thioredoxin system (cytoplasmic *trx-1*, cytoplasmic *trxr-1*, and mitochondrial *trxr-2*) to counteract the GSH deficiency.

In a previous study from our lab, GSH levels and SOD, glutathione peroxidase, and glutathione reductase activities were found not to change significantly following knockdown of *nadk-1*, although catalase activity was increased slightly (Gong 2022). As described above, in the thioredoxin redox system, a peroxiredoxin (thioredoxin peroxidase) becomes oxidized by H_2O_2 and then the peroxiredoxin gets reduced by thioredoxin, which becomes oxidized. Thioredoxin then gets reduced by thioredoxin reductase, dependent upon the oxidation of NADPH to $NADP^+$ (Jee et al. 2005). In *C. elegans,* the thioredoxin system is composed of ten genes, three peroxiredoxins, five thioredoxins and two thioredoxin reductases (Harris-Gauthier et al. 2022). These different proteins function in different tissues and subcellular localizations.

Thioredoxin-1 (TRX-1) and thioredoxin reductase-1 (TRXR-1) are expressed in the cytosol, with TRX-1 expressed exclusively in food-sensing, longevity-regulating ASJ neurons (Li et al.,2012). Thioredoxin-2 (TRX-2) and thioredoxin reductase-2 (TRXR-2) are expressed within the mitochondrial matrix (Li et al. 2012). Little is known regarding thioredoxins 3-5, but it has been shown that expression of *trx-3* is limited to the intestine (Harris-Gauthier et al. 2022). PRDX-2 is the major cytoplasmic peroxiredoxin, while PRDX-3 is the major mitochondrial peroxiredoxin. PRDX-6 is an atypical 1-Cys peroxiredoxin that is localized to both the cytoplasm and mitochondria (Ferguson and Bridge 2019).

During invertebrate evolution, thioredoxin reductase (TrxR) mutated to use a selenocysteine instead of a cysteine at its C-terminal active site (Boehler et al. 2013; Lacey and Hondal 2006). In *Drosophila melanogaster* due to the lack of a glutathione reductase gene, the TrxR enzyme reduces both thioredoxin and GSSG. The fruit fly TrxR enzyme retains the primordial cysteine residue at its active site and encodes both cytoplasmic and mitochondrial targeted splice isoforms (Lacey and Hondal 2006). *C. elegans* has two different TrxR genes, with cytoplasmic TRXR-1 containing a selenocysteine at the active site, while mitochondrial TRXR-2 contains a cysteine at that site (Boehler et al. 2013). Unlike thioredoxin reductases, *C. elegans* (and mammals) only possesses a single glutathione reductase gene GSR-1 with cytoplasmic and mitochondrial splice isoforms. Knockout of *C. elegans gsr-1* was shown to be lethal. Viability was restored by expressing the cytoplasmic, but not mitochondrial splice isoform (Mora-Lorca et al. 2016). Cytoplasmic GSR-1 is likely essential due to its role in larval cuticle shedding.

The cytoplasmic thioredoxin TRX-1 is required for normal *C. elegans* lifespan, while mitochondrial TRX-2 and TRXR-2 are required for the longevity of mitochondrial mutants.

Knockdown of *trxr-1* or *trxr-2*, but not *trx-1* or *trx-2* protected *C. elegans* from paraquat toxicity (Harris-Gauthier et al. 2022). However, another group working with mutant strains instead of RNAi-mediated gene knockdowns found that the *trxr-2(ok2267)* mutant showed protection against juglone, but not paraquat and that the *trx-2(tm2720)* mutant showed protection against both juglone and paraquat (Cacho-Valadez et al. 2012). Similar to the protection from paraquat or juglone toxicity described above, our lab found that knockdown of *nadk-1* or *nadk-2* protected from juglone toxicity (Gong 2022). With this in mind, we sought to test if there is an increase in *C. elegans* thioredoxin reductase activity following *nadk-1* knockdown that contributes to the juglone resistance.

Unlike humans that contain only one catalase gene that encodes a protein localized to peroxisomes, the *C. elegans* genome contains three catalase genes, with the *ctl-1* and *ctl-3* genes encoding cytoplasmic proteins. The *ctl-2* gene, encoding the peroxisomal catalase enzyme, has been shown to be the main source of worm catalase activity, providing roughly 80% of the total activity, and is likely the reason why only *ctl-2* deficiency, but not loss of *ctl-1* or *ctl-3*, results in decreased lifespan (Petriv and Rachubinski, 2004; Back et al. 2012). A heme group is present in the tertiary structure of catalase, which is important for catalase dismutation of H_2O_2 (Sepasi Tehrani and Moosavi-Movahedi 2018). Catalase has an interesting evolutionary history as the enzyme predates the atmospheric great oxidation event that occurred roughly two billion years ago (Olson et al. 2017). With catalase acting in parallel with the NADPH-fueled glutathione and thioredoxin systems, it seems logical that decreased GSH levels would result in increased catalase activity to counteract the increased ROS. Indeed, when the rate limiting enzyme of GSH synthesis, *gcs-1*, was knocked down, there was a roughly 25% increase in *ctl-1* expression. But even more important was the over 2-fold upregulation of the *trx-1*, *trxr-1*, and *trxr-2* genes of

the thioredoxin system to compensate for GSH depletion. Due to these compensatory mechanisms, knockdown of *gcs-1* starting from adulthood resulted in lifespan extension and paraquat resistance (Urban et al. 2017).

Use of *C. elegans* as a Model Organism

C. elegans is a hermaphroditic nematode (roundworm) found in the soil with 0.1% of the population being male. Adult nematodes are roughly a millimeter in length, transparent, and have a lifespan of roughly three weeks (at 20 °C). *C. elegans* is easy to maintain on a diet of *E. coli* or other bacteria (Labuschagne and Brenkman 2013). Because of its small size and transparency, *C. elegans* is amenable to microscopy without dissection (Zhang 2020). This transparency also has allowed for strains to be engineered that express fluorescent proteins targeted to specific tissues or cell types (Teschendorf and Link 2009). With a rapid life cycle of roughly 72 hours and a brood size of several hundred, *C. elegans* is able to rapidly produce high numbers of progeny. *C. elegans* hermaphrodites only possess 959 somatic cells. Despite this simplicity, they perform relatively complex behaviors for an organism with only 302 neurons. Their nervous system has evolved to respond to toxins, food, and mechanosensation (Giles and Rankin 2009).

In molecular aging research, the best model organisms to employ are those that are able to reproduce in large quantities, have short lifespans, and are easy to maintain. Traits such as these are useful when conducting experiments that require large amounts of individuals. *C. elegans* is thus an excellent model organism for aging research (Zhang et al 2020). With roughly 60% of the genes in their genome being homologous to human genes, *C. elegans* has been found to be a useful model in many studies related to human diseases and conditions. *C. elegans* completes four larval stages called L1 to L4 in around 48 hours before reaching adulthood.

Starvation causes L1 or L2 larvae to go into a hibernation state called dauer, which can be maintained for roughly 3 months, until food becomes available (Olsen et al. 2006). Entering the dauer state increases nematode resistance to stressful factors including heat, radiation, toxins, and oxidative stress.

C. elegans can be grown on agar plates or in liquid media. There is also a chemically defined liquid axenic medium that can be used as a diet instead of the normal bacterial diet. Therefore, *C. elegans* diet and culture environment can easily be manipulated. There are also tens of thousands of mutant strains available from the Ceanorhabditis Genetics Center. It is easy to knockdown the gene expression of a specific gene due to feeding RNAi technology and the availability of two global RNAi libraries that together cover roughly 90% of *C. elegans* genes. Gene knockdown by this feeding method is accomplished by feeding *C. elegans E. coli* containing a plasmid expressing RNA from opposite facing promoters to form double stranded RNA (dsRNA) that serves as a substrate for *C. elegans* RNA interference (RNAi) (Conte et al. 2015). The worms grind up the *E. coli* in their pharynx and absorb the dsRNA through their intestine and it spreads to most tissues with limited uptake by neurons (Timmons and Fire 1998). The *C. elegans* genome is also amenable to CRISPR-Cas9 genome editing (Olsen et al. 2006). Therefore, *C. elegans* is one of the top four eukaryotic model organisms used for genetic studies.

Strains Enabling Tissue-Specific Gene Knockdown by Feeding RNAi in *C. elegans*

Several strains of nematodes have been created where feeding them *E. coli* containing specific RNAi-plasmids can knockdown gene expression in a tissue-specific manner (Qadota et al. 2007). These strains typically have the *rde-1* component of the RNAi -induced silencing complex (RISC) knocked out and then a tissue-specific promoter is used to restore its expression

in only one tissue or cell-type. One such strain is VP303, where the *nhx-2* intestine-specific promoter is used to drive *rde-1* expression in the intestine. The VP303 strain also has a *rol6(su1006)* roller phenotype marker causing worms to move in a subtle axial motion. A similar strategy has been used for effective neuron-specific gene knockdown. In this case, the *sid-1* plasma membrane dsRNA transporter, which is expressed at very low levels in neurons, was knocked out globally and re-expressed specifically in neurons using the *unc-119* neuron-specific promoter yielding strain TU3401. These tissue- specific knockdown strains are fed the HT115(DE3) strain of *E. coli* containing an L4440 derived plasmid with phage T7 promoters flanking each side of a region of a *C. elegans* gene, such as *nadk-1*, to be knocked down. Administering IPTG to the *E. coli* induces the expression of the T7 polymerase to induce dsRNA production.

In *C. elegans*, two tissues known to have high metabolic demands are the neurons and the intestine. The nematode intestine shares many of the functions of mammalian liver and adipose. With high metabolic activity comes high production of ROS as a byproduct (Houthoofd et al. 2007). The use of a tissue-specific knockdown strain fed the *nadk-1* RNAi clone would yield a tissue-specific decrease in cytoplasmic NADK activity. In wild-type nematodes the GABAergic and dopaminergic neurons show resistance to RNAi compared to the cholinergic, glutamatergic, and touch neurons. Mutations in genes, such as *rrf-3* or *eri-1*, which increased the sensitivity of RNAi, increased the knockdown efficiency in all neuronal sub-types (Asikainen et al. 2005).

C. elegans and *nadk-1* Knockdown

As noted previously, *C. elegans* has two genes encoding NAD kinase enzymes, *nadk-1* and *nadk-2*. Some bioinformatic (Vickman and Erives 2019) and isolated mitochondrial

proteomic (Jing et al. 2009) evidence indicates that NADK-1 is localized to the cytoplasm, while NADK-2 is localized to the mitochondrial matrix. Experiments have yet to test for the presence of a cytoplasmically localized splice isoform of NADK-2 predicted by bioinformatic analysis. Previous research conducted by a former student in my lab investigated the effects of *nadk-1* or *nadk-2* knockdown in *C. elegans* on ROS levels in the presence of juglone and on nematode sensitivity to juglone toxicity (Gong 2022). In the presence of juglone it was found that, instead of increasing ROS levels as was expected, *nadk-1* or *nadk-2* knockdown decreased

ROS levels. In the absence of juglone *nadk-1* or *nadk-2* knockdown had no significant effect on *C. elegans* lifespan. However, knockdown of *nadk-2* in an *nadk-1* mutant strain led to a roughly 10% decreased lifespan. In addition, it was found that *nadk-1* knockdown had no effect on GSH levels or glutathione reductase, glutathione peroxidase, or SOD activity, while there was a tendency for increased *ctl-1* expression and a 2-fold increase in catalase activity. This led the investigator to hypothesize that increased catalase activity plays an important role in the decreased ROS levels observed following *nadk-1* knockdown. However, data from Chapter 3 in this thesis also suggest that decreased respiratory chain activity may be an additional factor causing decreased mitochondrial ROS production following *nadk-1* knockdown.

To determine if upregulation of *ctl-1* expression was the only factor responsible for the decreased ROS following *nadk-1* knockdown, the investigator performed experiments using a *ctl-1* mutant strain. A ROS assay using the ROS indicator dichlorodihydrofluorescein (H_2DCF) diacetate showed that the decreased ROS upon *nadk-1* knockdown was blocked in the *ctl-1* mutant. However, confirmation experiments using the H_2O_2-specific Amplex Red fluorescent indicator showed that *ctl-1* deficiency only partially blocked the decreased H_2O_2 following *nadk1* knockdown. Juglone toxicity experiments supported the results with Amplex Red. These

toxicity experiment results using the *ctl-1* mutant strain demonstrated that *nadk-1* knockdown still showed significant protection from juglone, although not as much protection was afforded as when knocking down *nadk-1* in the WT N2 strain. Thus, the investigator concluded that upregulation of the expression of the *ctl-1* catalase gene provided some of the protection against juglone in response to the depletion of cytoplasmic NADPH, but there were other molecular mechanisms that also contributed to the decreased ROS levels and protection from juglone toxicity.

In light of the results described above, I sought to perform additional H_2DCF diacetate ROS assays on nematodes in the absence or presence of *nadk-1* RNAi to determine the tissues that most greatly contribute to the decreased ROS levels when *nadk-1* was knocked down. I hypothesized there would be a greater decrease in ROS in tissues with the highest metabolic rates. Additionally, since double deficiency of *nadk-1* and *nadk-2* decreased lifespan, we wished to knockdown gene expression in tissues that most strongly regulate the rate of aging. Both of these criteria led to tissue-specific knockdown being performed in the intestine (using the VP303 strain) or the neurons (using the TU3401 strain). With the intestine being the most metabolically active tissue in nematodes, like the liver in mammals, and the tissue that most frequently signals for lifespan extension, we expected to observe a larger decrease in ROS when knocking down *nadk-1* in this tissue than in neurons. However, neurons are also a highly metabolically active cell type and can also signal for lifespan extension. So, we expected to observe some decrease in ROS levels when specifically knocking down *nadk-1* in neurons. To support the ROS measurements, O_2 consumption assays were performed under the same conditions to determine if there was a correlation between decreased ROS levels and decreased O_2 consumption. Finally, since there are three major cellular mechanisms to detoxify H_2O_2 and

the previous study only investigated catalase activity and the activities of glutathione reduction and peroxidation (Gong 2022), I chose to measure the activity of an enzyme in the thioredoxin branch of the H_2O_2 detoxification pathway. Therefore, a thioredoxin reductase activity assay was performed on the global and tissue-specific knockdowns. I expected to observe increases in thioredoxin reductase activity with both the global and intestine-specific knockdown of *nadk-1*.

CHAPTER 2. METHODS AND MATERIALS

Caenorhabditis elegans Strain Maintenance

C. elegans tissue-specific knockdown strain VP303 (*rde-1(ne219)* + [*nhx-2p::rde-1* + *rol-6(su1006)*]), which allows for gene knockdown by RNAi only in the intestine and TU3401 (*sid-1(pk3321)*+ [pCFJ90 (*myo-2p::mCherry*) + *unc-119p::sid-1*]), which allows for gene knockdown by RNAi only in neurons, were obtained from the Caenorhabditis Genetics Center (CGC, University of Minnesota). The tissue-specific knockdown strains, along with the WT N2 strain were grown on Nematode Growth Media (NGM) agar plates and maintained at 20°C. The tissue-specific knockdown strains, along with a s group of N2 nematodes, were fed HT115(DE3) *Escherichia coli* containing the L4440 plasmid with a portion of the *nadk-1* gene cloned between the phage T7 promoters, while another separate N2 group was fed HT115(DE3) *E. coli* containing an empty L4440 vector (EV) as a control.

E. coli Food Source Preparation

C. elegans were fed a diet of HT115(DE3) *E. coli* during the study. *E. coli* was cultured in lysogeny broth (LB) media consisting of 10 grams of tryptone, 5 grams of yeast extract, and 10 grams of NaCl added to a 2-liter flask followed by the addition of 1 liter of double deionized water. The contents were stirred until all solids were dissolved and then autoclaved. After autoclaving, the flask was placed into an ice bath until its temperature was near room temperature. Once cooled, 1 mM of IPTG, to induce expression of RNA from the L4440 plasmid, and 50 μg/mL of ampicillin to prevent growth of any contaminating bacteria, were added to the flask. IPTG was not added to the HT115(DE3) *E. coli* containing the empty L4440 vector (EV) used as the negative control. The culture media was then inoculated with *E. coli*

taken as a colony from an LB agar plate. The point of a pipette tip was used to remove cells from the colony that was grown on an LB agar plate. The pipette tip was injected into the culture medium in the flask. The other groups were given HT115(DE3) *E. coli* with the *nadk-1*containing insert in the L4440 plasmid. Following inoculation, the *E. coli* were grown by shaking the flask in an orbital shaking incubator set to 200 rpm and 37°C for 24 hours.

After the 24-hour culture, the *E. coli* suspension was poured into 500 mL centrifuge bottles with each bottle having an equal volume of culture suspension. The bottles were spun down at 3,075 x *g* for 10 minutes. Once spun down, the supernatant was removed and doubledeionized (ddI) water was added. The bottles were vortexed to resuspend the pellet and roughly 20 mL the *E. coli* suspension was poured into pre-weighed 50 mL conical centrifuge tubes. Each tube was filled to 35 mL with double deionized water and then spun down at 7,840 x *g* for 2 minutes. The supernatant was removed, more ddI water added, and the tube was vortexed to resuspend the pellet. The process was repeated two more times to fully wash the *E. coli*. The tube with the washed *E. coli* pellet was weighed again. The final tube weight was subtracted from the original empty tube weight to yield the mass of the *E. coli* pellet. ddI was added to yield a 100 mg/mL suspension. The tube was labelled and stored in a 4°C refrigerator for use within a month.

NGM Agar Plate Preparation

NGM agar plates were prepared according to standard protocol by adding 3 grams of NaCl, 17 grams of agar, and 2.5 grams of peptone to 1 L of ddI water. The solution was mixed thoroughly and autoclaved for 90 minutes (Stiernagle 2006). The autoclaved solution was placed in a 65°C water bath alongside solutions of 5 mg/mL cholesterol in ethanol, 1 M KPO_4, 1 M $MgSO_4$, and 1 M $CaCl_2$. Once all solutions were the same temperature, 1 mL of each was added

to the autoclaved solution, except for the 1 M KPO_4 solution, in which 25 mL was added. Next, 1 mL of a 1 M IPTG solution and 1 ml of a 50 mg/mL ampicillin solution was added. The final solution was vigorously mixed before immediately pouring 20 mL into each of roughly fifty 10 cm plastic petri dishes. The NGM agar was then left to solidify overnight before storing the plates at 4°C.

Age Synchronization

A mixed age population of *C. elegans* growing on 10 cm NGM agar plates for 3 or more days was used for the alkaline bleach synchronization as described in Porta-de-la-Riva et al. (2012). *C. elegans* and *E. coli* were washed from the plates with 0.1 M NaCl and transferred into four 50 mL tubes for each group and spun down at 769 x *g* for 2 minutes. The *E. coli* suspension was aspirated off down to 5 mL to avoid the centrifuged *C. elegans* pellet. The tubes were then filled back up to 50 mL with 0.1 M NaCl, and the process was repeated three times. After the third aspiration step, a solution of 5mL of 5M NaOH, 6.67 mL bleach, and 34mL ddI water was added. The solution damages adult (and larval) worm cuticles so that the nematodes lyse releasing the eggs. The eggs are more resistant to lysis due to their protective eggshell. The alkaline hypochlorite solution was mixed with 5 mL of worm suspension that had not been aspirated after the final wash step. The alkaline bleach-worm suspension was then placed on a rocker for approximately ten minutes, then centrifuged, and the supernatant was aspirated off as done previously to remove any remaining bleach, so as to not lyse the eggs. After three washes, the bleach was largely removed. Five 2 µL drops of egg-containing suspension were pipetted onto a glass slide and counted under a stereomicroscope. The average of the five measurements was used. On average roughly 10,000 eggs from each group were isolated. Roughly 10,000

eggs were then pipetted onto a new NGM agar plate along with 200 uL of a 100 mg/mL *E. coli* suspension containing the EV control or *nadk-1* knockdown clone.

Sucrose Flotation

After 48 hours at 20°C, the age synchronized nematodes developed to the L3-L4 stage, the developmental stage where the assays are routinely performed before the nematodes start laying eggs to disrupt the synchronization population. Before the worms were assayed they underwent a sucrose flotation protocol. This protocol not only removed *E. coli* attached to the worms, but also separated live worms from any dead nematodes that may have carried over from the bleach synchronization protocol. The worms were cleaned from their plates as previously described in the age synchronization section except the worms were transferred to 15 mL tubes instead of 50 mL tubes. After three washes, 5 mL of 0.1 M NaCl and 5 mL of a 60% sucrose solution were added and the tube was gently vortexed. The worms were then spun down in a centrifuge at 1,107 x *g* for 2 minutes. Live worms sedimented near the top of the sucrose gradient. With a separate transfer pipette for each group, the top live layer of worms was pipetted off into 50 mL tubes that were then topped off with 0.1 M NaCl to dilute any remaining sucrose. The washing protocol was repeated three times to remove all traces of sucrose. The final pellet was suspended in 5 mL of 0.1 M NaCl for the assays.

ROS Assay

ROS levels were assayed using 50 µM H_2DCF diacetate (Ewald et al., 2017). In each well of a 96-well plate (n=5), 200 µl of a suspension of 400 worms and 50 µM H_2DCF diacetate in 0.1 M NaCl were added. In each treatment group, 5 mM of tert-butyl hydroperoxide was also present. The DCF fluorescence (488 nm excitation, 528 nm emission) as an indicator of ROS

was then read every 15 minutes for 495 minutes using a Biotek Synergy 2 microplate reader. ROS levels were averaged over the five technical replicates and normalized to protein. Three biological replicates were performed.

Oxygen Consumption Assays

The rate of O_2 consumption was measured as described in Edwards et al., 2013, with modifications. 400 µl of worm sample containing roughly 800 worms in 0.1 M NaCl was added to a Clark O_2 electrode (Strathkelvin model MT200A) and measured for 15 minutes to obtain a steady rate of O_2 consumption loss from the chamber. The rate was normalized to worm protein.

Thioredoxin Reductase Activity Assay

Thioredoxin reductase activity was measured using an assay kit according to the manufacturer's instructions (Caymen Chemical Company), with slight modifications. Following a sucrose flotation, worms were immediately flash frozen and sonicated to release the soluble proteins. 1.75 mg of nematode protein was added to each well of a 96-well plate (n=3) together with kit components and the absorbance was read in a Biotek Synergy 2 microplate reader. Activity measurements were normalized to protein.

BCA Protein Quantification for ROS Assay, O_2 Consumption, and Thioredoxin Reductase Activity Assay

Protein quantification was performed after ROS assays, O_2 consumption assays, and thioredoxin reductase activity assays to normalize the results. A ThermoFisher Scientific Pierce BCA protein assay kit was used. For sample preparation, the method from Luz et al., was used with slight modifications. Worm samples were flash frozen in liquid nitrogen. After thawing, the nematodes were centrifuged at 2,200 x *g* for five minutes. The supernatant was removed without

affecting the worm pellet and replaced with 5 mL of 10% SDS. The samples were briefly chilled before being sonicated to avoid overheating the samples. The samples were sonicated at 3.0 seconds on, 9.0 seconds off intervals for 30 seconds at the lowest setting available using the Sonics VCX 750 sonicator. The sonication process was repeated on samples visually not thoroughly disrupted. The samples were then used according to the instructions in the BCA protein assay kit, substituting a 10% SDS solution for water. The absorbance of the samples was read at 562 nm using a Biotek Synergy 2 microplate reader. Protein concentrations in the samples were calculated by fitting them to the linear regression of the values of the standards.

Statistical Analysis

Statistical analysis was performed for all experiments using Sigma Plot software version 11. The ROS assays were performed three times, with each trial using five technical replicates. The O_2 consumption assays were performed three times, with each trial using four technical replicates. The thioredoxin reductase activity assays were performed three times, with each trial using two technical replicates. T-tests were used to determine statistical significance using $p < 0.05$. All data was analyzed for outliers. Differences between mean values were measured by one-way analysis of variance (ANOVA).

CHAPTER 3. RESULTS

ROS Assays

This study was undertaken in part to determine the effects of *nadk-1* knockdown on *C. elegans* ROS levels. A previous study showed that knockdown of several PPP enzymes starting from the L1 stage of larval development including *tald-1*, *tkt-1*, or T25B9.9 decreased NADPH levels and increased ROS to signal for lifespan extension (Bennett et al. 2017). But *nadk-1* knockdown did not increase lifespan, even though the [NADPH]/[$NADP^+$] ratio declined (Gong 2022). So, the molecular mechanisms for the lack of lifespan extension following *nadk-1* knockdown are being pursued. A previous study from my lab found that *nadk-1* or *nadk-2* knockdown decreased juglone-induced ROS levels (Gong 2022). But juglone, like the other redox cycling agents menadione, plumbagin, and paraquat (Bus & Gibson, 1984), oxidizes NADPH as part of the cycle to produce ROS (Klotz et al. 2014). So, the decreased ROS levels observed following NADK knockdown and juglone addition may have just been an artifact of decreased NADPH levels decreasing juglone-induced redox cycling. So, in this study tert-butyl hydroperoxide (t-BHP) was used as an inducer of ROS generation instead of juglone. As shown in Figure 3**,** similar to the results obtained following juglone treatment, global knockdown of *nadk-1* greatly decreased ROS levels in t-BHP treated L4 nematodes. Interestingly, specifically knocking down *nadk-1* in neurons or intestine was almost as potent in reducing ROS levels as the global knockdown. The reason for the non-linear increased ROS levels (DCF signal) over time in the WT *C. elegans* without gene knockdown is not known, but a similar response has also been observed by another lab (Yoon et al. 2018). This non-linear response was shown to be larger at lower H_2DCF diacetate indicator levels. Figure 4 shows a bar graph of the results taken at the 495-minute time point. A one-way ANOVA, $P<.001$, was run alongside the t-test

performed, as well as a post-hoc test, ($p < 0.05$). In both tests there was a significant difference between all comparisons, with the exception of the global *nadk-1* knockdown compared to the intestinal knockdown when using Tukey's post-hoc analysis ($q = 0.495$).

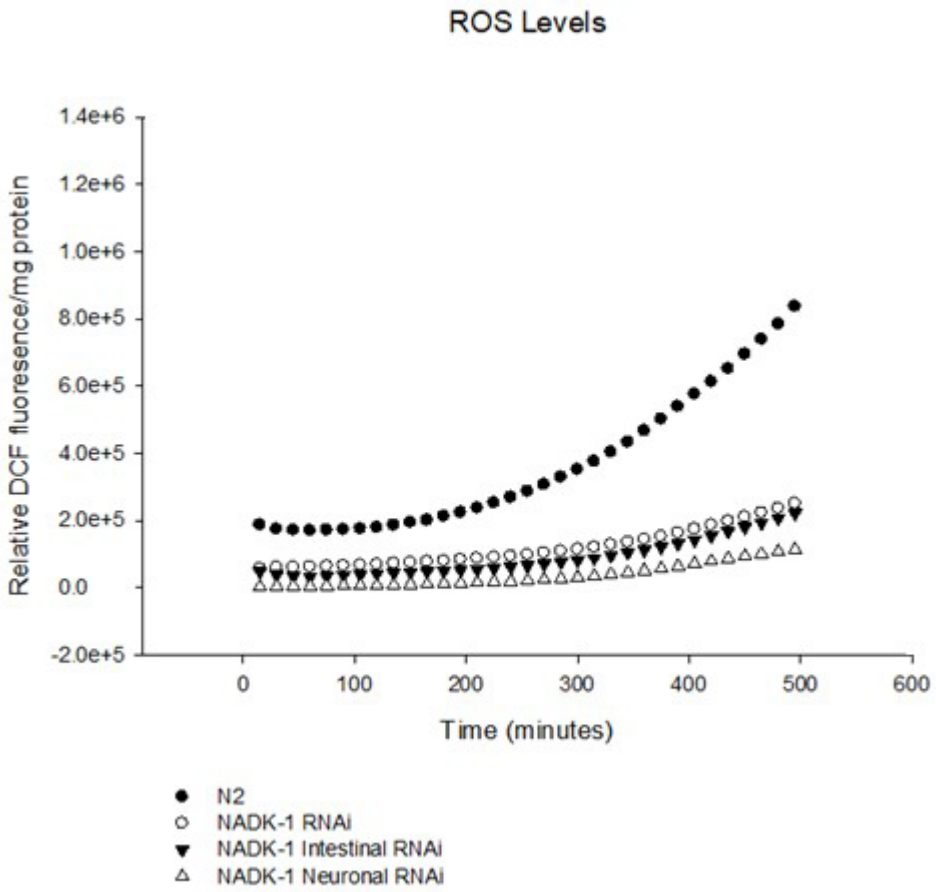

Figure 3. ROS Assay. Global, intestinal, or neuronal knockdown of *nadk-1* decreases t-BHP stimulated ROS levels. *C. elegans* nematodes at the L4 larval stage were used. 5 mM t-BHP was added at t=0 min. ROS measurements were taken every 15 minutes for 495 minutes.

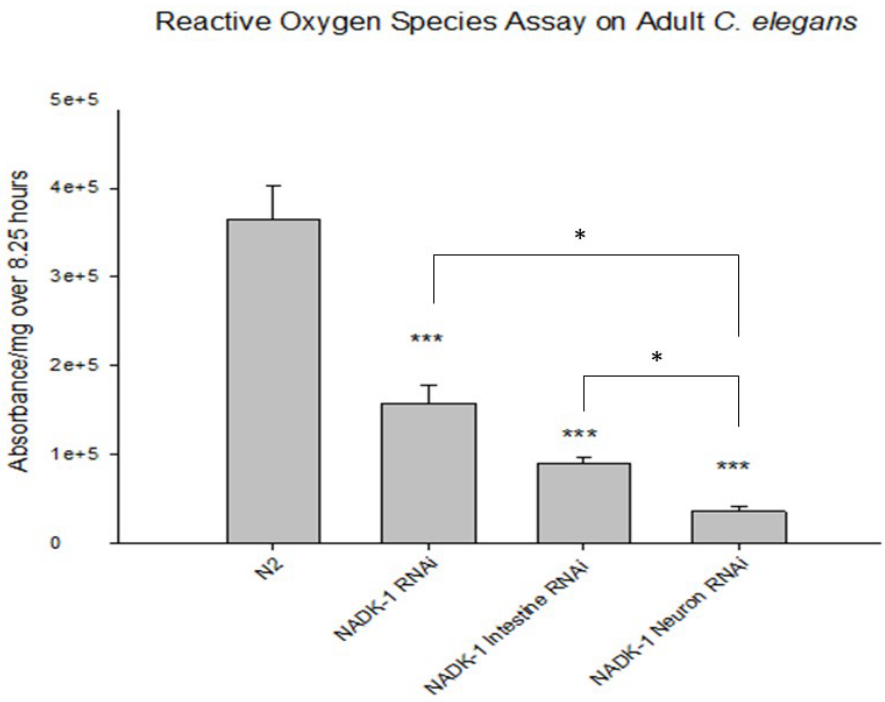

Figure 4. Effect of nadk-1 Knockdown on Tert-Butyl Hydroperoxide-Stimulated ROS levels. T-test and one-way ANOVA showing global, intestinal, or neuronal knockdown of *nadk-1* decreases t-BHP stimulated ROS levels 495 minutes after t-BHP addition. The conditions were the same as for Figure 1. *** indicates $p < 0.001$; * indicates $p < 0.05$

Oxygen Consumption Assays

The basal O_2 consumption rates were measured using the WT N2 strain, the intestinalspecific knockdown strain VP303, or the neuronal-specific knockdown strain TU3401, each fed the *nadk-1* RNAi clone, as well as the WT N2 strain fed the empty vector-containing *E. coli*. As shown in Figure 5**,** there was a significant 35-50% decrease in O_2 consumption in all *nadk-1* knockdown groups compared to the N2 empty vector-fed control. Following the t-test, a one-way analysis of variance between the groups was tested in the oxygen consumption experiments ($p < 0.001$) with a post-hoc test ($p < 0.05$). Results showed that while there was a significant difference between the N2 control group and the *nadk-1* knockdown groups, there were no significant differences between the knockdown groups.

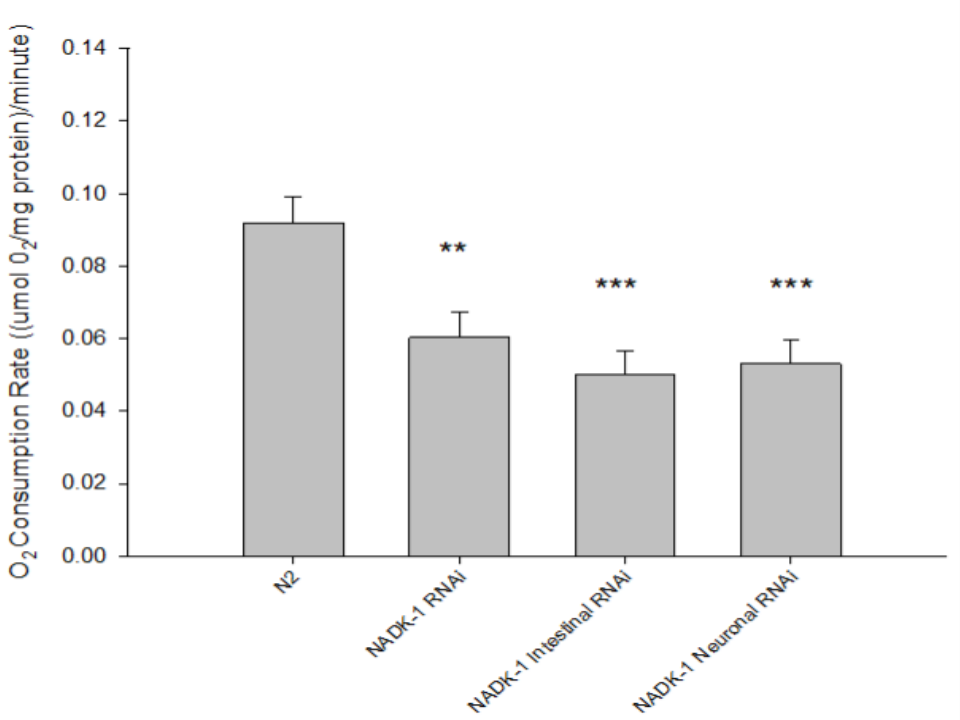

Figure 5. Effect of nadk-1 Knockdown on Basal Oxygen Consumption Rate. Global, intestinal, or neuronal knockdown of *nadk-1* decreased *C. elegans* O_2 consumption rate. L4 nematodes were used for the experiments. ** $p < 0.01$; *** $p < 0.001$.

Thioredoxin Reductase Activity Assays

Thioredoxin reductase activity levels were measured when *nadk-1* was knocked down starting from the L1 larval stage globally using N2 nematodes or when using the tissue-specific knockdown strains VP303 and TU3401. The results were compared to N2 wildtype nematodes feeding on empty vector-containing *E. coli* as shown in Figure 6. There was no significant difference in any of the *nadk-1* knockdown groups compared to the N2 control fed empty vector *E. coli*. However, there were non-significant trends toward increased thioredoxin reductase activity with the global or neuronal-specific knockdown of *nadk-1*.

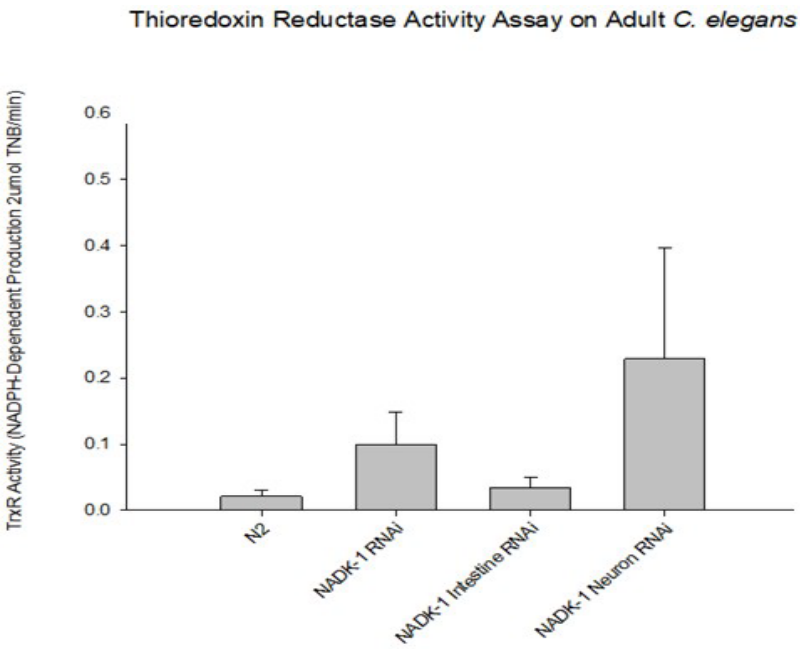

Figure 6. Effect of nadk-1 Knockdown on Thioredoxin Reductase Activity. T-test measuring thioredoxin reductase activity. No significant effects of knocking down *nadk-1* on *C. elegans* thioredoxin reductase activity ($p < 0.05$). The means and SEMs were calculated from three independent trials with two technical replicates per trial.

CHAPTER 4. DISCUSSION

ROS are a byproduct of mitochondrial metabolism and have been linked to a number of disorders including heart disease, neurodegeneration, cancer, and obesity as well as aging. Recent studies, however, have shown that a slight increase in ROS in young organisms can actually lead to compensatory mechanisms increasing lifespan. Superoxide, formed from the reduction of O_2 to $O_2^{\cdot-}$ by excessive leakage of electrons from electron transport chain complexes, is first detoxified by SODs to H_2O_2. H_2O_2 damages cellular components such as DNA, proteins, and lipids. NADPH is required for reducing cytoplasmic or mitochondrial H_2O_2 into water, specifically to recycle GSSG and the oxidized form of thioredoxin back to their reduced forms. In *C. elegans* decreased NADPH has also been shown to upregulate catalase activity as a compensatory response. Therefore, this study was designed to determine the effects of cytoplasmic *nadk-1* knockdown that decreases NADPH on mitochondrial respiratory function and cellular ROS levels.

Knockdown of *nadk-1* Decreases *C. elegans* O_2 Consumption Rate

C. elegans intestinal cells and neurons are highly metabolic cells with heavy mitochondrial demands. Therefore, mitochondria in these cells generate large amounts of ROS. Following *nadk-1* knockdown in these cells to decrease cytoplasmic NADPH levels, it was hypothesized that there would be decreased O_2 consumption as knockdown of the cytoplasmic PPP enzyme *tald-1* decreased NADPH levels that led to decreased O_2 consumption (Bennett et al. 2017). Therefore, my hypothesis was confirmed by the data. However, the molecular mechanism through which decreased cytoplasmic NADPH levels decrease mitochondrial O_2 consumption remains unresolved and is an active area of research in my lab.

One possibility is that the decreased O_2 consumption is a result of decreased cytoplasmic NADPH levels decreasing the rate of fatty acid synthesis leading to an increase in cytoplasmic acetyl-CoA and citrate levels (Figure 7). Fatty acids are primarily synthesized from mitochondrial citric acid cycle citrate that is exported into the cytoplasm using the *C. elegans* mitochondrial citrate transporter protein K11H3.3. Once in the cytoplasm the citrate reacts with coenzyme A (CoA) to form acetyl-CoA and oxaloacetate catalyzed by the *C. elegans* major ATP-citrate lyase enzyme ACLY-1 with the possible help of ACLY-2. For fatty acid synthesis acetyl-CoA and bicarbonate are converted to malonyl-CoA by the *C. elegans* enzyme acetylCoA carboxylase POD-2. *C. elegans* fatty acid synthase enzyme FASN-1 adds two carbons from malonyl-CoA to the end of a growing fatty acid chain with the release of the third carbon as carbon dioxide. FASN-1 catalyzes four enzymatic reactions for each two-carbon addition to the growing fatty acid chain with two of the reactions oxidizing NADPH to $NADP^+$ (enoyl-CoA reductase and ß-ketoacyl-ACP reductase). Therefore, decreased cytoplasmic NADPH would likely increase malonyl-CoA, acetyl-CoA, and citrate levels. As mentioned above, citrate is an inhibitor of the third enzyme of glycolysis, phosphofructokinase, which in turn would decrease the production and transport of pyruvate to the mitochondria to decrease O_2 consumption (Icard et al. 2021).

The increased cytoplasmic malonyl-CoA could also contribute to the decreased O_2 consumption by inhibiting the enzyme carnitine palmitoyl transferase (CPT-1, CPT-2, CPT-3, CPT-4, CPT-5, and CPT-6 in *C. elegans*), the rate limiting step of mitochondrial fatty acid betaoxidation (Foster 2012). CPT-2 and CPT-6 may be the most abundant *C. elegans* CPT isoforms as they were the only CPT proteins identified in a mitochondrial proteomics study (Jing et al. 2009). Carnitine palmitoyl transferase is localized to both the inner surface of the

outer mitochondrial membrane and to the inner surface of the inner mitochondrial membrane. In the outer membrane it converts fatty acyl-CoA to fatty acylcarnitine, which is exchanged for carnitine across the inner mitochondrial membrane. In the inner membrane carnitine palmitoyl transferase performs the reverse reaction to convert the fatty acylcarnitine back to fatty acylCoA, the substrate for beta-oxidation (Bonnefont et al. 2004). So, decreased carnitine palmitoyl transferase activity would decrease the rate of fatty acid beta-oxidation that produces NADH and $FADH_2$ for the electron transport chain. The final result would likely be a decreased rate of oxidative phosphorylation contributing to the decreased O_2 consumption observed.

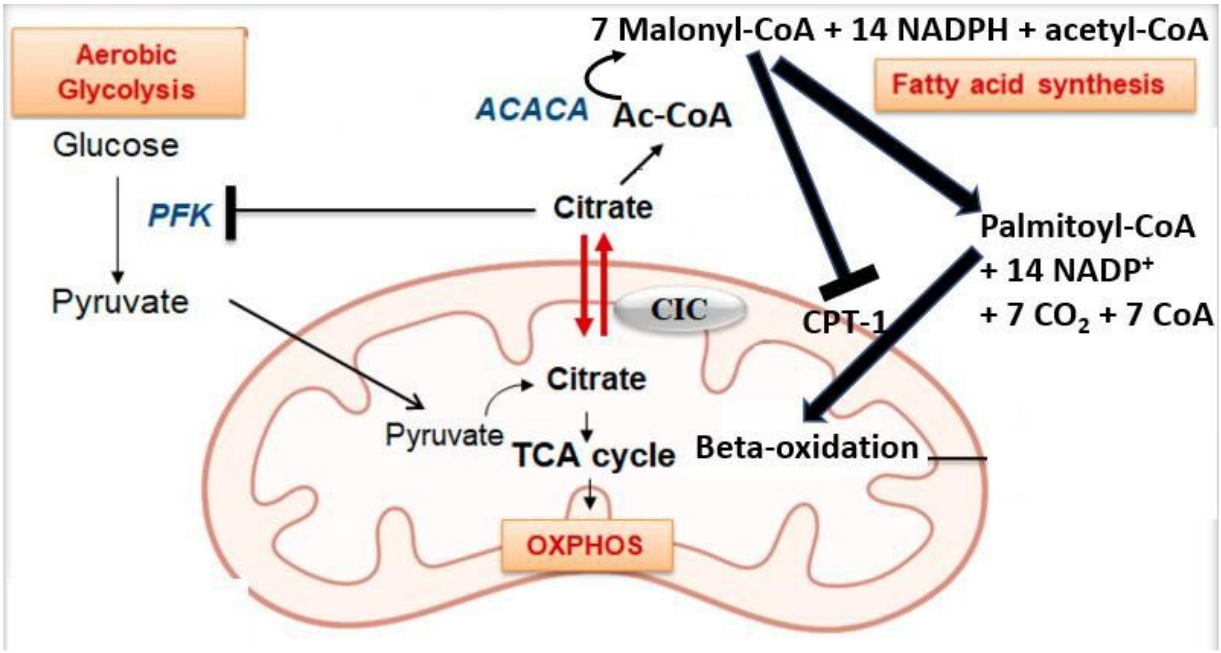

Figure 7. Inhibited Pyruvate Fatty Acid Oxidation Reduces O2 Consumption. Decreased NADPH likely leads to increased levels of citrate and malonyl-CoA, decreasing pyruvate levels and inhibiting fatty acid beta-oxidation, respectively, leading to decreased O_2 consumption.

Knockdown of *nadk-1* Decreases ROS levels

In this thesis it was shown that global, intestinal, or neuronal knockdown of *nadk-1* decreased *C. elegans* tBHP-induced ROS levels ($p < 0.001$). There are at least six highly used worm strains for tissue-specific knockdown. With the use of these strains, genes can be knocked down specifically in the intestine, neurons, hypodermis, germline, body wall muscle, or pharyngeal muscle. We found that knockdown of *nadk-1* decreased tBHP-induced ROS more in the neuronal-specific than the intestinal-specific knockdown or global knockdown strains. The mechanisms behind this effect are not easy to interpret. The most straightforward explanation may be that knockdown of *nadk-1* specifically in other cell types such as germline cells, hypodermal cells, or muscle cells increases tBHP-induced ROS levels, so that the effect of global knockdown is an additive effect from some tissues with increased and some tissues with decrease ROS levels that sum to be roughly as potent as intestine-specific or neuronal-specific knockdown. These results may also be explained in part by the low efficacy of neuronal knockdown in the N2 strain used for global knockdown, as neuronal-specific knockdown using the TU3401 strain showed the strongest ability to decrease ROS levels.

There are also *C. elegans* strains available to perform gene knockdown specifically in one-particular class of neurons including glutamatergic, GABAergic, cholinergic, or dopaminergic neurons. It would be interesting to determine which type of neuron contributes the most to the decreased ROS levels when *nadk-1* is knocked down. Another likely explanation for the stronger tissue-specific effects on ROS levels than that observed with the global knockdown is cell non-autonomous signaling effects. There is much inter-tissue communication in *C. elegans*, especially when it comes to stress and longevity signaling (H. A. Miller et al. 2020).

For example, decreased O_2 consumption in neurons could lead to the release of neuronal signaling molecules that bind to receptors on the plasma membrane of intestinal cells leading to decreased O_2 consumption in the intestinal cells as well. Also, it remains to be determined if the decreased ROS observed in the neuronal or intestinal-specific knockdown strains is partly due to a compensatory increase in catalase activity, similar to that reported for global *nadk-1* knockdown (Gong 2022).

Lastly, eukaryotic cells possess a reversible NADPH shuttle that allows for the transport of NADPH reducing equivalents across the mitochondrial inner membrane, even though NADP(H) itself is not transported. This NADPH shuttle relies upon the mitochondrial transport of citrate and the presence of reversible aconitase and NADP(H)-dependent isocitrate dehydrogenase enzymes in both the cytoplasm (ACO-1 and IDH-1) and mitochondrial matrix (ACO-2 and IDH-2). Therefore, it is possible that NADPH depletion in the cytoplasm results in NADPH depletion in the mitochondrial matrix. As mentioned earlier there are several mechanisms through which decreased mitochondrial matrix NADPH levels could decrease respiratory function including accumulation of the toxic lysine catabolite saccharopine (Zhou et al. 2019), decreased proline synthesis (Zhu et al. 2021), decreased beta-oxidation of unsaturated fatty acids, and decreased mitochondrial fatty acid synthesis required for electron transport chain complex assembly (Tanvir Rahman et al. 2023). Consistent with the requirement of NADPH for mitochondrial electron transport chain function, knockdown of the NADPH-oxidizing mitochondrial fatty acid synthesis gene *mecr-1* activates the *C. elegans* mitochondrial unfolded protein response (UPR^{mt}) commonly observed following electron transport chain gene knockdown (Rolland et al., 2019). However, knockdown of the lipoic acid synthetase gene (*lias-*

1) also activated UPR^{mt}. Since synthesis of lipoic acid, a cofactor for five mitochondrial enzymes, also requires mitochondrial 8-carbon fatty acid (octanoic acid) synthesis, decreased mitochondrial NADPH levels may activate UPR^{mt} by depleting lipoic acid rather than by decreasing electron transport chain complex assembly.

Knockdown of *nadk-1* Did Not Significantly Alter Thioredoxin Reductase Activity

As noted in the results, thioredoxin reductase activity was not significantly different following the global, intestinal-specific, or neuronal specific *nadk-1* knockdown compared to the control, although trends toward increased activity were found for the global and neuronalspecific knockdowns. There were high levels of variability among assay replicates yielding large error bars. The inter-assay variability may have been due in part due to not adding a protease inhibitor cocktail to the *C. elegans* before their lysis by flash freezing and sonication. Different amounts of thioredoxin reductase may have been proteolyzed in the different biological replicates.

It is unknown if the thioredoxin reductase kit sold to assay the mammalian seleniumdependent thioredoxin reductases TRXR1 and TRXR2 will be able to detect the activity of the *C. elegans* selenium-independent mitochondrial TRXR-2 enzyme. As both glutathione reductase and thioredoxin reductases reduce the DTNB substrate used in the assay to the TNB product measured by absorbance, the assay kit makes use of the mammalian thioredoxin reductase inhibitor aurothiomalate to subtract off the portion of the TNB product absorbance synthesized independently of thioredoxin reductase (presumably by glutathione reductase). It is unknown if *C. elegans* TRXR-2 is inhibited by aurothiomalate. If aurothiomalate is not an inhibitor of TRXR-2, the results only display the change in activity of the *C. elegans* cytoplasmic TRXR-1. Since there was much variability between the different

trials when using the neuronal-specific knockdown strain, more replicates are needed to determine if more consistent data can be obtained.

Different Effects on ROS Levels When Knocking Down NADKs Versus Knocking Down $NADP^+$-Reducing Enzymes When Both Likely Decrease NADPH Levels

One of the largest questions posed by this research is why does knocking down NADKs decrease tBHP-induced ROS levels when it was shown that knocking down PPP enzymes to decrease NADPH levels increased endogenous ROS levels (Bennett et al. 2017). To answer that question, measurements of endogenous ROS with *nadk-1* knockdown without tBHP added should be performed. It is not likely that *nadk-1* knockdown in the absence of tBHP increases ROS levels. Another possible explanation is that mitochondrial ROS production is sensitive to the cytoplasmic [NADPH]/[$NADP^+$] ratio. Knocking down $NADP^+$-reducing enzymes such as PPP enzymes will slightly decrease the cytoplasmic [NADPH]/[$NADP^+$] ratio leading to increased ROS, while knocking down cytoplasmic *nadk-1* likely decreases both [NADPH] and [$NADP^+$] levels that could lead to a different effect on the magnitude of the [NADPH]/[$NADP^+$] ratio. Knocking down the PPP gene *tald-1* decreased the NADPH/$NADP^+$ by roughly 2-fold (Bennett et al. 2017). It would be helpful if the nematode [NADPH]/[$NADP^+$] ratio is measured in future studies of *nadk-1* knockdown to attempt to confirm this hypothesis.

Conclusion

This study showed that knocking down *C. elegans nadk-1* decreased O_2 consumption and tBHP-induced ROS levels. The decreased electron transport chain activity may be leading to decreased mitochondrial ROS production. Therefore, the increased catalase activity measured following *nadk-1* knockdown (Gong 2022) is likely not the only mechanism responsible for the decreased ROS levels measured. Decreased cytoplasmic NADPH may be leading to reduced

glycolytic and carnitine palmitoyl transferase activity decreasing the import of pyruvate and fatty acids into the mitochondrial matrix and their rate of oxidation. O_2 consumption and ROS measurements using WT and *nadk-1* mutant strains with fatty acid synthase (*fasn-1*), acetyl-CoA carboxylase (*pod-2*), ATP-citrate lyase (*acly-1*), or mitochondrial citrate carrier (K11H3.3) knockdown are needed to confirm or refute the proposed molecular mechanism.

Future Studies and Limitations of the Current Study

To determine the mechanisms through which *nadk-1* or *nadk-2* knockdown decrease O_2 consumption and ROS levels, the following experiments could be conducted in the future:

- O_2 consumption and H_2DCF diacetate ROS assays could be performed using *C. elegans* WT N2 and *nadk-1* mutant strains feeding knockdown clones to the mitochondrial citrate transporter K11H3.3, ATP-citrate lyase ACLY-1, acetyl-CoA carboxylase POD-2, or fatty acid synthase FASN-1.
- Citrate, acetyl-CoA, and malonyl-CoA levels as well as carnitine palmitoyl transferase activity and pyruvate dehydrogenase activity could be measured following *nadk-1* knockdown
- Knockdown *C. elegans* mitochondrial *nadk-2* and determine the effects on O_2 consumption and ROS levels and perform tissue-specific knockdown experiments as performed in this study.

The current study has several limitations including not measuring ROS in the absence of tBHP, not using the Amplex Red H_2O_2-specific fluorescent indicator for ROS measurements, and not measuring O_2 consumption and ROS levels using isolated mitochondria.

Personal limitations include the steep learning curve that I encountered when I joined the lab and the long length of time it took me to learn the bioenergetics and metabolism-based experimental techniques due the minimal biochemistry knowledge I had when entering. Once I finally learned the techniques there was not much time left to perform the experiments to test my hypothesis. I look forward for others to follow up on my results to test if decreased NADPH levels contributes to organismal aging and if maintaining or slightly increasing NADPH levels extends lifespan.

REFERENCES

Alfadda AA, Sallam RM. 2012. Reactive oxygen species in health and disease. J Biomed Biotechnol. 2012. doi:10.1155/2012/936486.

Aquilano K, Baldelli S, Ciriolo MR. 2014. Glutathione: New roles in redox signalling for an old antioxidant. Front Pharmacol. 5 AUG. doi:10.3389/fphar.2014.00196.

Asikainen S, Vartiainen S, Lakso M, Nass R, Wong G. 2005. Selective sensitivity of Caenorhabditis elegans neurons to RNA interference. Neuroreport. 16(18). doi:10.1097/00001756-200512190-00005.

Babior BM. 2004. NADPH oxidase. Curr Opin Immunol. 16(1). doi:10.1016/j.coi.2003.12.001.

Back P, Braeckman BP, Matthijssens F. 2012. ROS in aging Caenorhabditis elegans: Damage or signaling? Oxid Med Cell Longev. doi:10.1155/2012/608478.

Bayr H. 2005. Reactive oxygen species. Crit Care Med. 33(Suppl):S498–S501. doi:10.1097/01.CCM.0000186787.64500.12.

Bennett CF, Kwon JJ, Chen C, Russell J, Acosta K, Burnaevskiy N, Crane MM, Bitto A, Vander Wende H, Simko M, et al. 2017. Transaldolase inhibition impairs mitochondrial respiration and induces a starvation-like longevity response in Caenorhabditis elegans. PLoS Genet. 13(3):e1006695. doi:10.1371/journal.pgen.1006695.

Boehler CJ, Raines AM, Sunde RA. 2013. Deletion of Thioredoxin Reductase and Effects of Selenite and Selenate Toxicity in Caenorhabditis elegans. PLoS One. 8(8). doi:10.1371/journal.pone.0071525.

Bonnefont JP, Djouadi F, Prip-Buus C, Gobin S, Munnich A, Bastin J. 2004. Carnitine palmitoyltransferases 1 and 2: Biochemical, molecular and medical aspects. Mol Aspects Med. 25(5–6). doi:10.1016/j.mam.2004.06.004.

Bradshaw PC. 2019. Cytoplasmic and mitochondrial NADPH-coupled Redox systems in the regulation of aging. Nutrients. 11(3). doi:10.3390/nu11030504.

Braeckman BP, Houthoofd K, De Vreese A, Vanfleteren JR. 2002. Assaying metabolic activity in ageing Caenorhabditis elegans. In: Mechanisms of Ageing and Development. Vol. 123.

Bus JS, Gibson JE. 1984. Paraquat: model for oxidant-initiated toxicity. Environ Health Perspect. 55. doi:10.1289/ehp.845537.

Cabreiro F, Ackerman D, Doonan R, Araiz C, Back P, Papp D, Braeckman BP, Gems D. 2011. Increased life span from overexpression of superoxide dismutase in Caenorhabditis elegans is not caused by decreased oxidative damage. Free Radic Biol Med. 51(8). doi:10.1016/j.freeradbiomed.2011.07.020.

Cacho-Valadez B, Muñoz-Lobato F, Pedrajas JR, Cabello J, Fierro-González JC, Navas P, Swoboda P, Link CD, Miranda-Vizuete A. 2012. The characterization of the caenorhabditis elegans mitochondrial thioredoxin system uncovers an unexpected protective role of thioredoxin reductase 2 in β-Amyloid peptide toxicity. Antioxid Redox Signal. 16(12). doi:10.1089/ars.2011.4265.

Chandrasekaran A, Idelchik M del PS, Melendez JA. 2017. Redox control of senescence and age-related disease. Redox Biol. 11. doi:10.1016/j.redox.2016.11.005.

Chatterji A, Sachin K, Sengupta R. 2022. Glutathione-dependent thioredoxin reduction and lipoamide system support in-vitro mammalian ribonucleotide reductase catalysis: a possible antioxidant redundancy. Mol Biol Rep. 49(8):8179–8183. doi:10.1007/s11033-022-07480-4.

Chesney J. 2006. 6-Phosphofructo-2-kinase/fructose-2,6-bisphosphatase and tumor cell glycolysis. Curr Opin Clin Nutr Metab Care. 9(5):535–539. doi:10.1097/01.mco.0000241661.15514.fb.

Ciccarese F, Ciminale V. 2017. Escaping Death: Mitochondrial Redox Homeostasis in Cancer Cells. Front Oncol. 7. doi:10.3389/fonc.2017.00117.

Conte D, MacNei LT, Walhout AJM, Mello CC. 2015. RNA Interference in Caenorhabditis elegans. Curr Protoc Mol Biol. 2015. doi:10.1002/0471142727.mb2603s109.

Cypser JR, Johnson TE. 2002. Multiple Stressors in Caenorhabditis elegans Induce Stress Hormesis and Extended Longevity. J Gerontol A Biol Sci Med Sci. 57(3):B109–B114. doi:10.1093/gerona/57.3.B109.

Ding CKC, Rose J, Sun T, Wu J, Chen PH, Lin CC, Yang WH, Chen KY, Lee H, Xu E, et al. 2020. MESH1 is a cytosolic NADPH phosphatase that regulates ferroptosis. Nat Metab. 2(3). doi:10.1038/s42255-020-0181-1.

Edwards CB, Copes N, Brito AG, Canfield J, Bradshaw PC. 2013. Malate and Fumarate Extend Lifespan in Caenorhabditis elegans. PLoS One. 8(3). doi:10.1371/journal.pone.0058345.

Ewald C, Hourihan J, Blackwell T. 2017. Oxidative Stress Assays (arsenite and tBHP) in Caenorhabditis elegans. Bio Protoc. 7(13). doi:10.21769/bioprotoc.2365.

Fernandez-Marcos PJ, Nóbrega-Pereira S. 2016. NADPH: New oxygen for the ROS theory of aging. Oncotarget. 7(32). doi:10.18632/oncotarget.10744.

Foster DW. 2012. Malonyl-CoA: The regulator of fatty acid synthesis and oxidation. Journal of Clinical Investigation. 122(6). doi:10.1172/JCI63967.

Giles AC, Rankin CH. 2009. Behavioral and genetic characterization of habituation using Caenorhabditis elegans. Neurobiol Learn Mem. 92(2). doi:10.1016/j.nlm.2008.08.004.

Gladyshev VN. 2014. The free radical theory of aging is dead. Long live the damage theory! Antioxid Redox Signal. 20(4). doi:10.1089/ars.2013.5228.

Gong H. 2022. Knockdown of C. elegans NAD Kinases NADK-1 or NADK-2 Induces an Antioxidant Response Without Affecting Lifespan.

Goodman RP, Calvo SE, Mootha VK. 2018. Spatiotemporal compartmentalization of hepatic NADH and NADPH metabolism. Journal of Biological Chemistry. 293(20). doi:10.1074/jbc.TM117.000258.

HARMAN D. 1972. The Biologic Clock: The Mitochondria? J Am Geriatr Soc. 20(4). doi:10.1111/j.1532-5415.1972.tb00787.x.

Harris-Gauthier N, Traa A, AlOkda A, Moldakozhayev A, Anglas U, Soo SK, Van Raamsdonk JM. 2022. Mitochondrial thioredoxin system is required for enhanced stress resistance and extended longevity in long-lived mitochondrial mutants. Redox Biol. 53:102335. doi:10.1016/j.redox.2022.102335.

Houthoofd K, Gems D, Johnson T, Vanfleteren J. 2007. Dietary restriction in the nematode Caenorhabditis elegans. Interdiscip Top Gerontol. 35. doi:10.1159/000096558.

Icard P, Coquerel A, Wu Z, Gligorov J, Fuks D, Fournel L, Lincet H, Simula L. 2021. Understanding the central role of citrate in the metabolism of cancer cells and tumors: An update. Int J Mol Sci. 22(12). doi:10.3390/ijms22126587.

Jee C, Vanoaica L, Lee J, Park BJ, Ahnn J. 2005. Thioredoxin is related to life span regulation and oxidative stress response in Caenorhabditis elegans. Genes to Cells. 10(12). doi:10.1111/j.1365-2443.2005.00913.x.

Jing L, Tanxi C, Peng W, Ziyou C, Xiulan C, Junjie H, Zhensheng X, Peng X, Linan S, Pingsheng L, et al. 2009. Proteomic analysis of mitochondria from Caenorhabditis elegans. Proteomics. 9(19). doi:10.1002/pmic.200900101.

Ju H-Q, Lin J-F, Tian T, Xie D, Xu R-H. 2020. NADPH homeostasis in cancer: functions, mechanisms and therapeutic implications. Signal Transduct Target Ther. 5(1):231. doi:10.1038/s41392-020-00326-0.

Klotz LO, Hou X, Jacob C. 2014. 1,4-naphthoquinones: From oxidative damage to cellular and inter-cellular signaling. Molecules. 19(9). doi:10.3390/molecules190914902.

Li W, Bandyopadhyay J, Hwaang HS, Park BJ, Cho JH, Lee J Il, Ahnn J, Lee SK. 2012. Two thioredoxin reductases, trxr-1 and trxr-2, have differential physiological roles in caenorhabditis elegans. Mol Cells. 34(2). doi:10.1007/s10059-012-0155-6.

Liochev SI. 2013. Reactive oxygen species and the free radical theory of aging. Free Radic Biol Med. 60. doi:10.1016/j.freeradbiomed.2013.02.011.

Luz AL, Smith LL, Rooney JP, Meyer JN. 2015. Seahorse Xf ^{e} 24 Extracellular Flux Analyzer-Based Analysis of Cellular Respiration in *Caenorhabditis elegans*. Curr Protoc Toxicol. 66(1). doi:10.1002/0471140856.tx2507s66.

Miinalainen IJ, Schmitz W, Huotari A, Autio KJ, Soininen R, Van Themaat EVL, Baes M, Herzig KH, Conzelmann E, Hiltunen JK. 2009. Mitochondrial 2,4-dienoyl-CoA reductase deficiency in mice results in severe hypoglycemia with stress intolerance and unimpaired ketogenesis. PLoS Genet. 5(7). doi:10.1371/journal.pgen.1000543.

Miller CG, Holmgren A, Arnér ESJ, Schmidt EE. 2018. NADPH-dependent and -independent disulfide reductase systems. Free Radic Biol Med. 127. doi:10.1016/j.freeradbiomed.2018.03.051.

Miller HA, Dean ES, Pletcher SD, Leiser SF. 2020. Cell non-autonomous regulation of health and longevity. Elife. 9. doi:10.7554/ELIFE.62659.

Mora-Lorca JA, Sáenz-Narciso B, Gaffney CJ, Naranjo-Galindo FJ, Pedrajas JR, Guerrero-Gómez D, Dobrzynska A, Askjaer P, Szewczyk NJ, Cabello J, et al. 2016. Glutathione reductase gsr-1 is an essential gene required for Caenorhabditis elegans early embryonic development. Free Radic Biol Med. 96. doi:10.1016/j.freeradbiomed.2016.04.017.

Morris D, Ly J, Chi PT, Daliva J, Nguyen T, Soofer C, Chen YC, Lagman M, Venketaraman V. 2014. Glutathione synthesis is compromised in erythrocytes from individuals with HIV. Front Pharmacol. 5 APR. doi:10.3389/fphar.2014.00073.

Nassar ZD, Mah CY, Dehairs J, Burvenich IJG, Irani S, Centenera MM, Helm M, Shrestha RK, Moldovan M, Don AS, et al. 2020. Human decr1 is an androgen-repressed survival factor that regulates pufa oxidation to protect prostate tumor cells from ferroptosis. Elife. 9. doi:10.7554/eLife.54166.

Nguyen KT, Mun S-H, Yang J, Lee J, Seok O-H, Kim E, Kim D, An SY, Seo D-Y, Suh J-Y, et al. 2022. The MARCHF6 E3 ubiquitin ligase acts as an NADPH sensor for the regulation of ferroptosis. Nat Cell Biol. 24(8):1239–1251. doi:10.1038/s41556-022-00973-1.

Oliveira RP, Abate JP, Dilks K, Landis J, Ashraf J, Murphy CT, Blackwell TK. 2009. Condition-adapted stress and longevity gene regulation by Caenorhabditis elegans SKN-1/Nrf. Aging Cell. 8(5). doi:10.1111/j.1474-9726.2009.00501.x.

Olsen A, Vantipalli MC, Lithgow GJ. 2006. Using Caenorhabditis elegans as a model for aging and age-related diseases. In: Annals of the New York Academy of Sciences. Vol. 1067.

Olson KR, Gao Y, DeLeon ER, Arif M, Arif F, Arora N, Straub KD. 2017. Catalase as a sulfide-sulfur oxido-reductase: An ancient (and modern?) regulator of reactive sulfur species (RSS). Redox Biol. 12. doi:10.1016/j.redox.2017.02.021.

Patra KC, Hay N. 2014. The pentose phosphate pathway and cancer. Trends Biochem Sci. 39(8):347–354. doi:10.1016/j.tibs.2014.06.005.

Petriv OI, Rachubinski RA. 2004. Lack of Peroxisomal Catalase Causes a Progeric Phenotype in Caenorhabditis elegans. Journal of Biological Chemistry. 279(19):19996–20001. doi:10.1074/jbc.M400207200.

Porta-de-la-Riva M, Fontrodona L, Villanueva A, Cerón J. 2012. Basic Caenorhabditis elegans methods: Synchronization and observation. Journal of Visualized Experiments.(64). doi:10.3791/4019.

Qadota H, Inoue M, Hikita T, Köppen M, Hardin JD, Amano M, Moerman DG, Kaibuchi K. 2007. Establishment of a tissue-specific RNAi system in C. elegans. Gene. 400(1–2). doi:10.1016/j.gene.2007.06.020.

Radak Z, Zhao Z, Koltai E, Ohno H, Atalay M. 2013. Oxygen consumption and usage during physical exercise: The balance between oxidative stress and ROS-dependent adaptive signaling. Antioxid Redox Signal. 18(10). doi:10.1089/ars.2011.4498.

Rolland SG, Schneid S, Schwarz M, Rackles E, Fischer C, Haeussler S, Regmi SG, Yeroslaviz A, Habermann B, Mokranjac D, et al. 2019. Compromised Mitochondrial Protein Import Acts as a Signal for UPRmt. Cell Rep. 28(7). doi:10.1016/j.celrep.2019.07.049.

Ronchi JA, Francisco A, Passos LAC, Figueira TR, Castilho RF. 2016. The Contribution of Nicotinamide Nucleotide Transhydrogenase to Peroxide Detoxification Is Dependent on the Respiratory State and Counterbalanced by Other Sources of NADPH in Liver Mitochondria. Journal of Biological Chemistry. 291(38):20173–20187. doi:10.1074/jbc.M116.730473.

Salisbury D, Bronas U. 2015. Reactive oxygen and nitrogen species: Impact on endothelial dysfunction. Nurs Res. 64(1). doi:10.1097/NNR.0000000000000068.

Sepasi Tehrani H, Moosavi-Movahedi AA. 2018. Catalase and its mysteries. Prog Biophys Mol Biol. 140. doi:10.1016/j.pbiomolbio.2018.03.001.

Speakman JR, Selman C. 2011. The free-radical damage theory: Accumulating evidence against a simple link of oxidative stress to ageing and lifespan. BioEssays. 33(4). doi:10.1002/bies.201000132.

Stiernagle T. 2006. Maintenance of C. elegans. WormBook. doi:10.1895/wormbook.1.101.1.

Tanvir Rahman M, Kristian Koski M, Panecka-Hofman J, Schmitz W, Kastaniotis AJ, Wade RC, Wierenga RK, Kalervo Hiltunen J, Autio KJ. 2023. An engineered variant of MECR reductase reveals indispensability of long-chain acyl-ACPs for mitochondrial respiration. Nat Commun. 14(1):619. doi:10.1038/s41467-023-36358-7.

Teschendorf D, Link CD. 2009. What have worm models told us about the mechanisms of neuronal dysfunction in human neurodegenerative diseases? Mol Neurodegener. 4(1). doi:10.1186/1750-1326-4-38.

Timmons L, Fire A. 1998. Specific interference by ingested dsRNA [10]. Nature. 395(6705). doi:10.1038/27579.

Urban N, Tsitsipatis D, Hausig F, Kreuzer K, Erler K, Stein V, Ristow M, Steinbrenner H, Klotz LO. 2017. Non-linear impact of glutathione depletion on C. elegans life span and stress resistance. Redox Biol. 11. doi:10.1016/j.redox.2016.12.003.

Vickman O, Erives A. 2019. Episodic evolution of a eukaryotic NADK repertoire of ancient provenance. PLoS One. 14(8). doi:10.1371/journal.pone.0220447.

Xu M, Ding L, Liang J, Yang X, Liu Y, Wang Y, Ding M, Huang X. 2021. NAD kinase sustains lipogenesis and mitochondrial metabolismthrough fatty acid synthesis. Cell Rep. 37(13). doi:10.1016/j.celrep.2021.110157.

Xu Z, Jing K, Liu Y, Cen P. 2006. High-level expression of recombinant glucose dehydrogenase and its application in NADPH regeneration. J Ind Microbiol Biotechnol. 34(1):83–90. doi:10.1007/s10295-006-0168-2.

Yoon D, Lee M-H, Cha D. 2018. Measurement of Intracellular ROS in Caenorhabditis elegans Using 2',7'-Dichlorodihydrofluorescein Diacetate. Bio Protoc. 8(6). doi:10.21769/bioprotoc.2774.

Zhang R, Zhang K. 2023. Mitochondrial NAD kinase in health and disease. Redox Biol. 60:102613. doi:10.1016/J.REDOX.2023.102613.

Zhou J, Wang X, Wang M, Chang Y, Zhang F, Ban Z, Tang R, Gan Q, Wu S, Guo Y, et al. 2019. The lysine catabolite saccharopine impairs development by disrupting mitochondrial homeostasis. Journal of Cell Biology. 218(2). doi:10.1083/jcb.201807204.

Zhu J, Schwörer S, Berisa M, Kyung YJ, Ryu KW, Yi J, Jiang X, Cross JR, Thompson CB. 2021. Mitochondrial NADP(H) generation is essential for proline biosynthesis. Science (1979). 372(6545). doi:10.1126/science.abd5491.

VITA

JAKE A. REGAN

Education:	B.S. Psychology, King University, Bristol, Tennessee, USA, 2021
	M.S Biomedical Science, East Tennessee State University, Johnson City, Tennessee, USA, 2023
Personal Experience	Graduate Teaching Assistant, East Tennessee State University, Tennessee, USA, 2021-2023
	Teaching Assistant, King University, Bristol, Tennessee, USA, 2020-2021